AIAA JOURNAL
Vol. 33, No. 4, April 1995

Torsional Actuation with Extension-Torsion Composite Coupling and a Magnetostrictive Actuator

Christopher M. Bothwell,* Ramesh Chandra,† and Inderjit Chopra‡
University of Maryland, College Park, Maryland 20742

This paper presents an analytical-experimental study of using magnetostrictive actuators in conjunction with an extension-torsion coupled composite tube to actuate a rotor blade trailing-edge flap to actively control helicopter vibration. Thin-walled beam analysis based on Vlasov theory was used to predict the induced twist and extension in a composite tube with magnetostrictive actuation. To validate the analysis, extension-torsion coupled Kevlar®-epoxy tubes of different ply lay-ups were fabricated using an autoclave molding technique. These tubes were first tested under static mechanical loads, and tip twist and axial extension were measured by means of a laser optical system and strain gages, respectively. Good correlation between theory and experiment was achieved. Subsequently, these composite tubes were tested under magnetostrictive actuation. The $[11]_2$ Kevlar-epoxy tube system generated the maximum twist, 0.19 deg in tension and 0.20 deg in compression. The Kevlar-epoxy systems showed good correlation between measured and predicted twist values. Finally, alternate actuator concepts for these tubes, specifically piezoelectric stacks and electrostrictive actuators, were examined, and a piezoelectric stack actuator was found to induce much larger force and twist (approximately 3 times that created by the magnetostrictive actuator/tube system).

Nomenclature

D	= inner diameter of composite tube
F	= axial force applied to composite tube
F_{block}	= block force of actuator
K_{ij}	= stiffness matrix of composite tube
ℓ	= length of composite tube
M_z, M_{zs}	= moment resultants referring to plate segment of tube
N	= axial force referring to tube
N_z, N_{zs}	= stress resultants referring to plate segment of tube
T_s	= torsion moment referring to tube
W	= axial displacement of tube
W_{actuator}	= axial displacement of actuator
W_{free}	= free axial displacement of actuator
W_{tube}	= axial displacement of tube
ε_s, ε_z, ε_{sz}	= strains in plate segment of tube
ε_{xz}, ε_{yz}	= transverse shear strains of tube
ϕ_x, ϕ_y, ϕ_z	= rotations of tube about x, y, z axes
φ	= warping function
κ_s, κ_z, κ_{sz}	= bending curvatures referring to plate segment of tube
σ_s, σ_z, σ_{sz}	= stress field referring to plate segment of tube

Introduction

RECENTLY, active control of helicopter vibrations has received considerable attention from researchers. These vibrations are caused by unsteady aerodynamic forces occurring at a dominant frequency of $N\Omega$, where N is the number of blades and Ω is the rotational speed. The concept of higher harmonic control (HHC) has been investigated as a possible method of actively suppressing helicopter vibration.[1] HHC reduces helicopter vibration through excitation of the blade pitch at higher harmonics of the rotational speed. The changes in blade pitch generate new unsteady airloads that act to cancel out the blade loads that caused the original vibration. A common method of HHC relies on multicyclic blade pitch control by means of swash plate actuation. However, the swash plate actuation is restricted to frequencies that are integral multiples of the rotor blades. Therefore, with a HHC system, it is not possible to excite other frequencies that are important for rotor performance and blade life. The frequency limitation of the swash plate can be overcome with individual blade control (IBC). The IBC concept, developed by Ham et al.,[2] employs actuators on individual blades in the rotating frame with independent control of each rotor blade; thus the actuation frequency is not limited to integer multiples of $N\Omega$. However, there is a mechanical complexity of hydraulic sliprings with an IBC system.

Straub and Robinson[3] presented an analytical study of an IBC system using a trailing-edge flap concept to actively control rotor noise caused by blade vortex interaction (BVI). The study modeled the dynamics of both the rotor and the individual flap actuation. Results showed that nonharmonic flap inputs induced significant elastic torsion responses at 1, 5, and 6 rev^{-1}. These responses can substantially increase oscillatory blade section loads and therefore may be used to reduce helicopter vibration and/or noise. Currently, a one-fourth model scale AH-64 rotor is being developed for a proof of concept test. Dawson and Straub[4] have completed the design, component testing, and hover testing of an active flap model rotor for further study of reduction of BVI noise and suppression of blade vibration. The flap is driven by a cable located along the blade's elastic axis attached to a cam follower at the hub. During testing, the flap was operated mechanically to generate the highest possible flap deflection. Mach-scaled hover tests were performed in a wide range of conditions and were validated by advanced dynamic, aerodynamic, and acoustic analyses that predicted the effect of the flap on the blade torsional moments and elastic twist. Future research will include validation of performance and predictions in the NASA Langley 14 × 22-ft subsonic wind tunnel. Subsequently, Straub and Merkley[5] performed a feasibility study on the use of a servo-flap with on-blade smart material actuators for both primary and active rotor control. The study proposed the use of a hybrid stack/tube actuator consisting of a combination of piezoelectric stack and magnetostrictive stack actuators for use in cyclic and active control, coupled with a composite actuator tube embedded with shape memory alloy fibers for control of the collective pitch. The study concluded that, by optimizing the rotor and

Presented as Paper 94-1760 at the AIAA/ASME/ASCE/AHS/ASC 35th Structures, Structural Dynamics, and Materials Conference, Hilton Head, SC, April 18–20, 1994; received June 28, 1994; revision received Sept. 23, 1994; accepted for publication Sept. 23, 1994.

*Graduate Research Assistant; currently at Bell Helicopter Textron. Member AIAA.

†Assistant Research Scientist, Center for Rotorcraft Education and Research, Department of Aerospace Engineering. Senior Member AIAA.

‡Professor and Director, Center for Rotorcraft Education and Research, Department of Aerospace Engineering. Fellow AIAA.

flap design parameters (based on size requirements for the AH-64 helicopter) in order to reduce the control loads and motions, the smart actuator system could generate the deflections necessary for rotor control.

Chopra and his group[6–8] are investigating the use of piezoceramic technology for vibration suppression in IBC systems . Two different piezoelectric actuation mechanisms being explored are blade twist induced by embedded piezoceramics and trailing-edge flap actuation by means of piezoelectric bender elements. Chen and Chopra[6,7] presented an experimental study of a dynamically scaled rotor blade embedded with piezoceramic elements for the purpose of vibration control. Banks of piezoelectric crystals at ±45 deg angles were embedded into the top and bottom surfaces of the blade. Equal and in-phase potentials were applied to the top and bottom piezoelectric elements inducing a twist distribution along the blade. Testing of a 6-ft-diameter Froude-scaled rotor model on the hover test facility showed that the magnitude of twist achieved was approximately 20 times less than the twist needed for significant vibration control of the rotor. Samak and Chopra[8] performed a feasibility study on the development of a Froude-scaled rotor model to suppress vibration by means of trailing-edge flap actuation. Here the flap was actuated by piezoceramic "bimorphs" (two piezoelements with a brass shim in the middle). If opposite potentials are applied to each element, a pure bending motion is caused. Through the use of a hinge-and-leverage arrangement, the bending motion generated by three bimorphs lined up side by side induced amplified deflection of the trailing-edge flap. Dynamic testing of the rotor on the hover stand showed flap deflections of the order of 2 deg at a tip speed of 258 ft/s (rpm = 900), approximately one-quarter of the deflection necessary for significant vibration suppression (a flap deflection of the order of ±8 deg is needed to effectively reduce vibration). Currently, improved bimorphs are being incorporated into this model to increase the flap deflection.[9] Major limitations with both these approaches are low actuator force and small induced displacement.

The use of magnetostrictive elements in a blade trailing-edge flap design was investigated by Fenn et al.[10] In this analytical study, pairs of magnetostrictive terfenol-D rods were mechanically linked to a control rod in a Y configuration where tension or compression induced in the terfenol-D caused linear motion of the control rod. Since the control rod was attached to a trailing-edge flap, the strain in the magnetostrictive elements induced actuation of the flap. This study was based on the UH-60A helicopter, and the theory predicted that three pairs of magnetostrictive rods driving four flaps per blade would provide the ±2 deg total blade deflection necessary to effectively reduce helicopter vibration. However, an experimental validation of this study has yet to be carried out.

This paper examines the concept of using magnetostrictive actuators in conjunction with an extension-torsion coupled tube to actuate the twisting motion of a trailing-edge flap. Figure 1 shows a schematic drawing of this concept. The axial force generated by a magnetostrictive actuator induces elastic twist in the coupled composite tube. This concept is especially suited for full-scale applications as the twist induced in the tube increases with length. This study focuses on the development of a methodology to predict the twist and axial deflection in an extension-torsion coupled composite tube actuated by a linear magnetostrictive, piezoelectric stack, or electrostrictive device. Beam theory developed in Ref. 11 is used to predict the axial-force-induced twist in a thin-walled coupled composite tube. Then, composite tubes are fabricated, followed by testing under mechanical loads as well as magnetostrictive-induced actuation to validate both the analysis and actuation concept. Finally, based on results of the magnetostrictive actuator/tube tests and analysis, some possible alternate actuator concepts are discussed.

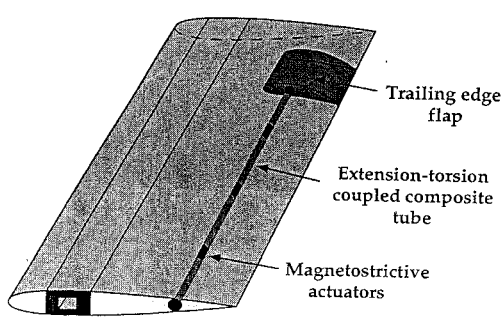

Fig. 1 Schematic of trailing-edge flap actuation using extension-torsion coupled composite tubes and linear actuators.

Analysis

In this paper, the beam analysis presented in Ref. 11 is specialized to predict the axial displacement and induced twist of an extension-torsion coupled composite circular cylindrical tube due to an axial force. The thin-walled analysis takes into account effects of transverse shear, section warping (Saint Venant torsion), and constrained warping at the edges (Vlasov torsion). The essence of this analysis is that two-dimensional stress and displacement fields associated with any shell segment of the tube are reduced to the generalized one-dimensional beam displacements and forces (Vlasov theory).

In-plane warping of the cross section is neglected and both the surface normal strain ε_s and normal stress σ_s are assumed small compared to the axial strain ε_z and axial stress σ_z, respectively. Thus, the nonzero strains and bending curvatures for a shell segment are ε_z, ε_{sz}, κ_z, and κ_{sz}. These are given as (see Ref. 11 for details)

$$\varepsilon_{sz} = \varepsilon_{xz}\cos\theta + \varepsilon_{yz}\sin\theta + \varepsilon_{sz}^{(s)} \tag{1}$$

$$\varepsilon_z = W' + x\phi_x' + y\phi_y' - \varphi\phi_z'' \tag{2}$$

$$\kappa_z = -\phi_x'\sin\theta + \phi_y'\cos\theta - \phi'' q_z + \varepsilon_{xz}'\sin\theta - \varepsilon_{yz}'\cos\theta \tag{3}$$

$$\kappa_{zs} = -2\phi_z' \tag{4}$$

The stress and moment resultants associated with a generic shell segment of the tube are

$$\begin{aligned} N_z &= A_{11}\varepsilon_z + A_{16}\varepsilon_{zs} + B_{11}\kappa_z + B_{16}\kappa_{zs} \\ N_{zs} &= A_{16}\varepsilon_z + A_{66}\varepsilon_{zs} + B_{16}\kappa_z + B_{66}\kappa_{zs} \\ M_z &= B_{11}\varepsilon_z + B_{16}\varepsilon_{zs} + D_{11}\kappa_z + D_{16}\kappa_{zs} \\ M_{zs} &= B_{16}\varepsilon_z + B_{66}\varepsilon_{zs} + D_{16}\kappa_z + D_{66}\kappa_{zs} \end{aligned} \tag{5}$$

Using relations (5) and the energy principle, the force-displacement relations of the composite tube are obtained (see Ref. 11 for details). These relations for the extension-torsion coupled tube are

$$\begin{Bmatrix} N \\ T_s \end{Bmatrix} = \begin{bmatrix} K_{11} & K_{15} \\ K_{15} & K_{55} \end{bmatrix} \begin{Bmatrix} W' \\ \phi_z' \end{Bmatrix} \tag{6}$$

where K_{11}, K_{15}, and K_{55} are, respectively, the extension, extension-torsion, and torsion stiffness coefficients as defined in Ref. 11. The axial displacement and induced twist at the tip in a thin uniform tube under an applied axial force are obtained using relations (6) and are given as

$$W = \frac{K_{55}}{K_{11}K_{55} - K_{15}^2} F\ell \tag{7}$$

$$\phi_z = \frac{K_{15}}{K_{11}K_{55} - K_{15}^2} F\ell \tag{8}$$

where F is the applied force and ℓ is the length of the composite tube.

Relations (7) and (8) are utilized to predict the response of an extension-torsion coupled tube under an applied mechanical load. To predict the twist and extension of this tube under any linear actuator (magnetostrictive, electrostrictive, and piezoelectric stacks), the force-displacement relation of the actuator were included in the composite tube analysis.

The force F and displacement W of the magnetostrictive actuator for a known excitation voltage are represented in linear form as

$$F = F_{\text{block}}\left(1 - \frac{W}{W_{\text{free}}}\right) \tag{9}$$

To include the actuator characteristics into the analysis of the combined actuator/tube system, it is assumed that the axial displacement of the actuator equals the corresponding axial extension in the composite tube, i.e.,

$$W_{\text{actuator}} = W_{\text{tube}} = W \tag{10}$$

By combining Eqs. (7–10), the axial extension of the composite tube system becomes

$$W = \frac{K_{55} F_{\text{block}} W_{\text{free}} \ell}{\left(K_{11}K_{55} - K_{15}^2\right) W_{\text{free}} + K_{55} F_{\text{block}} \ell} \tag{11}$$

Using relations (7) and (8), the induced twist is

$$\phi_z = \frac{K_{15}}{K_{55}} W \tag{12}$$

Design Study of Composite Tube

Induced twist in an extension-torsion coupled composite tube actuated by a magnetostrictive device depends on the material, ply lay-up, geometry of the tube, and the force-displacement characteristics of the actuator. Hence, this design study is aimed at determining the optimum design parameters for maximum induced twist and axial force. First, glass-epoxy, Kevlar®-epoxy, and graphite-epoxy materials were examined for maximum twist of a tube with fixed geometry under a unit axial, external load. Figure 2 shows the induced twist in Kevlar-epoxy, graphite-epoxy, and glass-epoxy composite tubes of 35 in. length, 1.57 in. diam, and 0.02 in. thickness, subjected to unit axial external load. It is evident from this figure that Kevlar-epoxy is the best suited material for this study as it provides the maximum twist for a prescribed force. Note that the maximum twist corresponds to 30 deg ply angle. However, the tubes with this ply angle will have excessive residual twist caused by curing temperatures. Hence, a thermally stable lay-up, $[20/-70]_s$, that causes minimum twist due to curing temperature was selected as a baseline configuration.[12]

Second, a parametric study is carried out for Kevlar-epoxy tubes actuated by the magnetostrictive device. For these calculations, an actuator with the block force of 190 lb and free displacement of 1.25 mils is considered. Tip twist and induced forces are calculated using relations (9), (11), and (12). Figure 3 shows the influence of ply angle on tip twist in Kevlar-epoxy tubes with fixed actuator and varying number of plies. The length and diameter of these tubes are held constant: length 34.375 in. and diameter 1.57 in. It is seen from this figure that a tube with two plies and 11 deg ply angle produces the maximum induced twist. Note that this ply angle corresponding to maximum twist is different from the ply angle obtained for a known axial force (Fig. 2). Also, the Kevlar-epoxy tube with $[11]_2$ lay-up will generate a maximum twist of 0.20 deg, about twice the twist generated by thermally stable baseline lay-up. Figure 4 presents the influence of ply angle on induced force for Kevlar-epoxy tubes with varying number of plies. The plot shows a decrease of force with increasing ply angle up to about 50 deg, at which the force levels off to a steady value. Also, the force in the $[11]_2$ Kevlar-epoxy composite tube assembly increases from 15 lb to almost 60 lb with a change of the number of plies from 2 to 8. Note that the induced force for the baseline configuration and $[11]_2$ lay-up is 15 lb.

Figures 5 and 6 illustrate the influence of length on the performance of the Kevlar-epoxy tubes in terms of twist and force for a fixed diameter (1.57 in.) and actuator. This effect is examined for tubes with $[11]_2$, $[11]_4$, and $[20/-70]_8$ ply lay-ups. It is seen from Fig. 5 that twist increases with the tube length; the increase is large initially, and becomes small later. Note that for $[11]_2$ lay-up tube, twist levels off to a value of 0.22 deg for a tube length of 90 in. Figure 6 shows that the actuator-induced force decreases rapidly with length of the tube, becoming less than 20 lb for all three cases at tube lengths greater than 60 in. It is seen from this figure that the baseline, thermally stable configuration has a twist magnitude approximately one-half of the $[11]_2$ lay-up, whereas the baseline system's induced force is equal to that of the $[11]_2$ Kevlar-epoxy tube system.

Figures 7 and 8 present the influence of diameter on induced twist and axial force of the tube with the length held constant at 34.375 in.

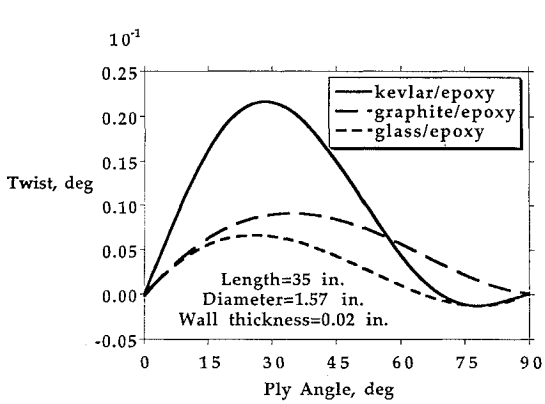

Fig. 2 Influence of ply angle on tip twist of composite tube under unit axial load.

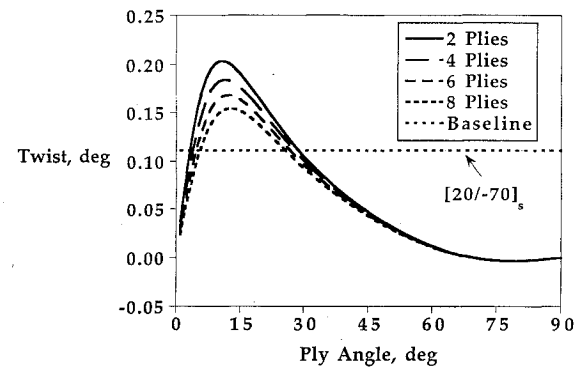

Fig. 3 Influence of ply angle on tip twist of Kevlar-epoxy tube with actuator (l = 34.375 in., D = 1.57 in.).

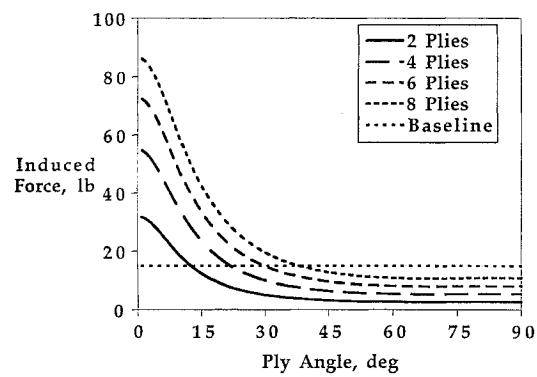

Fig. 4 Influence of ply angle on axial force of Kevlar-epoxy tube with actuator (l = 34.375 in., D = 1.57 in.).

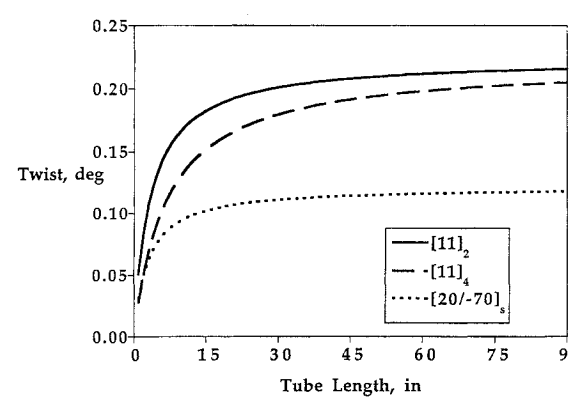

Fig. 5 Influence of tube length on tip twist of Kevlar-epoxy tube with actuator (D = 1.57 in.).

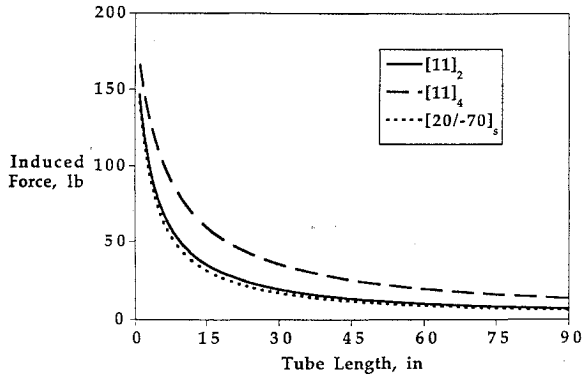

Fig. 6 Influence of tube length on axial force of Kevlar-epoxy tube with actuator (D = 1.57 in.).

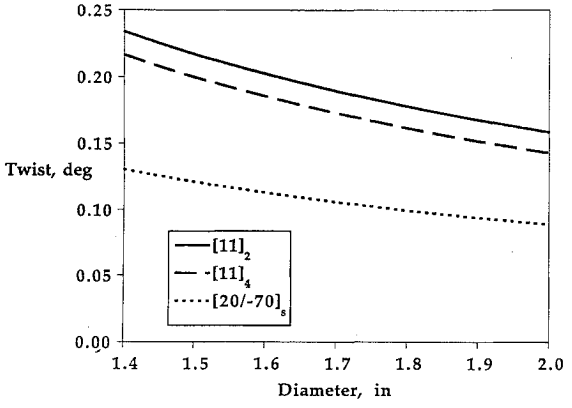

Fig. 7 Influence of tube diameter on tip twist of Kevlar-epoxy tube with actuator (l = 34.375 in.).

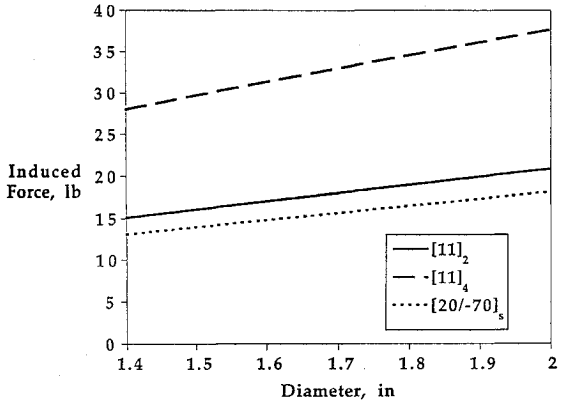

Fig. 8 Influence of tube diameter on axial force of Kevlar-epoxy tube with actuator (l = 34.375 in.).

and the above actuator force-displacement characteristics utilized. Once again, this effect is examined for tubes with $[11]_2$, $[11]_4$, and $[20/-70]_8$ ply lay-ups. The inner diameter is limited to 1.4 in. because the outer diameter of the magnetostrictive actuator is 1.34 in. Figure 7 shows that, as the tube diameter becomes larger, the tip twist decreases almost linearly with a maximum value of 0.23 deg for the $[11]_2$ composite tube system. From Fig. 8, a linear increase in induced force with increasing tube diameter is seen. Here the highest force case corresponds to the $[11]_4$ lay-up, about 38 lb at a diameter of 2 in. In both figures, the thermally stable system has the lowest twist and force values.

In a full-scale trailing-edge flap application, in addition to a high induced twist, a large force in the tube is desired to counteract the aerodynamic forces exerted on the flap. From the results, it is clear that the requirements for maximum twist and force conflict. Therefore, to determine the optimum composite tube system design, a multiobjective function study must be performed where both the tip twist and induced force are maximized.

Experiments

Fabrication of Composite Tubes

The Kevlar-epoxy composite tubes are fabricated using an autoclave molding technique. Unidirectional prepregs are laid up on the split metal mold shown in Fig. 9. The plies are sealed into a vacuum bag and a pump is used for further compacting of the layers. After laminating the desired number of plies, peel ply is wrapped to provide surface finish to the tube. Bleeder, breather, and barrier plies are added to control epoxy flow during the cure process. The lay-up is again sealed in a vacuum bag and cured in a microprocessor-controlled autoclave. The cure cycle given by the prepeg manufacturer is used. At the end of the cure, the lay-up is removed from the autoclave. Finally, the vacuum bag is removed and the tube is released from the mold.

Two end pieces are attached to the composite tube using a low-melting-point alloy that liquefies at approximately 158°F and resolidifies at room temperature. The end pieces are necessary to mechanically link the tube to the actuator assembly as well as to fix one end of the tube for external load tests. The twist of the tube is measured using a laser optical system. One end of the tube is bolted to a rectangular aluminum bar secured in a vise. External force is applied to the free end of the tube by means of a pulley and dead weight. The laser beam is reflected off a small mirror attached to the free end of the tube approximately 30 ft onto a wall. Displacement of the beam on the wall is converted to twist using trigonometric relations. In this particular setup, laser dot displacement of 1.0 in. on the wall corresponds to 0.083 deg of induced twist in the tube. The axial extension of the composite tube is measured using a pair of precision strain gages aligned along the longitudinal axis of the tube. The composite tube is allowed to hang free and dead weight is again used to apply an external axial load. The strain gages are bonded to diametrically opposite surfaces of the tube to eliminate any bending-induced strain in the response and axial displacement is calculated from this axial strain. The induced tip twist of the thermally stable tube is measured for external loads of up to 100 lb in increments of 10 lb. In the extension tests, dead weight is applied in 20-lb increments to 100 lb. The extension test is repeated four times to ensure data accuracy.

Force-Displacement Characteristics of Free Magnetostrictive Actuator

Figure 10 shows the schematic of a magnetostrictive actuator. This actuator has the capability of bidirectional motion. The actuator consists of a terfenol-D rod surrounded by an electric coil. An electric current in the coil induces a magnetic field that causes electrostriction of the terfenol-D. The permanent magnet introduces an initial strain to the rod allowing the actuator to compress when a negative direct current (dc) is applied. Note that this actuator also uses prestressing to enhance the performance of the terfenol-D. This actuator was tested in tension (positive dc) and compression (negative dc).

Testing of Composite Tube Under Mechanical Load

The force-displacement relation of a free actuator plays a very important role in the present application. Figure 11 shows a simple set-up, designed and fabricated to determine these characteristics of the present actuator. A lever arm is used to amplify the axial displacement of the actuator. The load is applied by means of dead

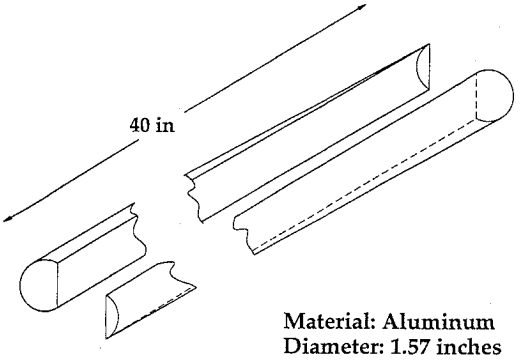

Fig. 9 Split mold for fabrication of composite tube.

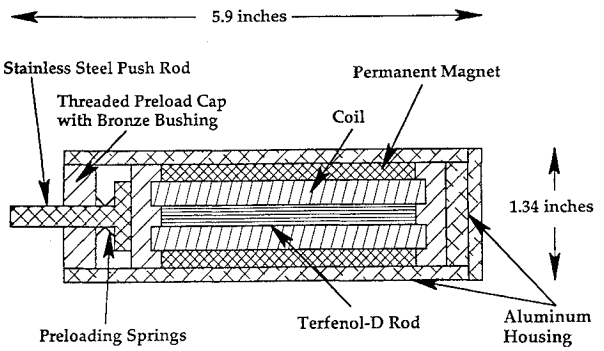

Fig. 10 Schematic of a magnetostrictive actuator.

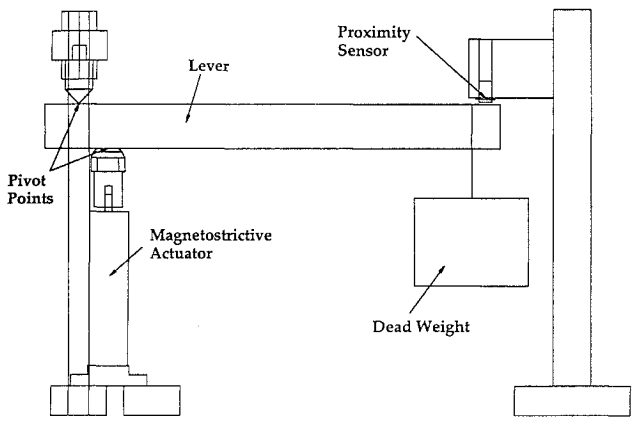

Fig. 11 Test set-up for determining force-displacement relation of actuator.

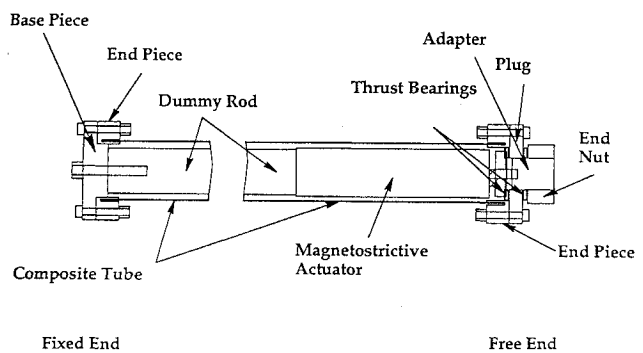

Fig. 12 Schematic of composite tube and actuator assembly.

weight, and a proximity sensor is used to measure deflection at the end of the lever arm, taking advantage of the amplification of the actuator motion. The force and displacement of the actuator are calculated using the known applied weight and measured deflection along with the lever ratio.

Testing of Coupled Composite Tube with Magnetostrictive Actuator

In order to utilize the extension-torsion coupling characteristics of the composite tube, the magnetostrictive actuator was attached to the tube in such a manner that both twist and axial displacement were allowed. Figure 12 shows the schematic drawing of the composite tube and actuator assembly. In this design, two end pieces are integrally connected to the ends of the composite tube by means of a low-melting-point alloy. A dummy rod is used to connect the actuator to the 34.375-in.-long Kevlar-epoxy tubes. On the fixed end of the tube assembly, the base is bolted to the tube end piece, whereas a separate bolt secures the dummy rod to the base piece, keeping the end rigidly constrained. At the tip of the magnetostrictive actuator (i.e., the push rod) an adapter with an end nut lengthens the push rod allowing for the addition of two thrust bearings and a plug. These bearings are essential to the design as they allow the plug to rotate freely when the magnetostrictive actuator applies an axial force to the system. Since the plug is bolted to the tube end piece, the composite tube will twist as the plug rotates. One end of the tube/actuator assembly is bolted to a rectangular aluminum bar secured in a vise. The twist and extension of the tube are again determined using the laser optical system and strain gages, respectively.

Results and Discussion

Composite Tubes under Mechanical Load

Figure 13 shows tip twist produced by externally applied axial load for the $[20/-70]_s$ Gevlar-epoxy cantilevered tube of 34.375 in. length, 1.57 in. diam and 0.04 in. thickness. Predictions for the tubes correlate well with measured values. Figure 14 shows axial displacement under this external load for the same baseline Kevlar-epoxy tube. Predicted longitudinal extensions for the Kevlar-epoxy tubes are within 20% of the experimental measurements. The wrinkles that occur during the manufacturing of the Kevlar tube may be the cause for the difference between theory and experiment.

Force-Displacement Relation of Magnetostrictive Actuator

Figure 15 shows the force-displacement characteristics of this actuator for electric currents of 1.0 A(4.0 V) and 1.5 A(6.0 V). Note that 1.5 A is the maximum input current recommended by the manufacturer. A line of best fit is drawn to the data to determine F_{block} and W_{free} for the 1.5-A case, and the tests are repeated to ensure consistency. From this figure the actuator block force is estimated to be about 190 lb and the free displacement is approximately 1.25 mils (10^{-3} in.) for a current of 1.5 A.

Structural Response of Composite Tube with Actuator

Figure 16 shows the tip twist of $[20/-70]_s$ and $[11]_2$ Kevlar-epoxy composite tubes induced by the actuator. The $[20/-70]_s$ Kevlar-epoxy tube system produced twists of 0.089 deg in tension and 0.102 deg in compression. Both values are close to the predicted twist of 0.111 deg, within 20 and 10%, respectively. This twist corresponds to an axial force of 11 lb in tension and 12 lb in compression. For the $[11]_2$ tube system, the induced twists of 0.19 deg in tension and 0.2 deg in compression are obtained, and the correlation between

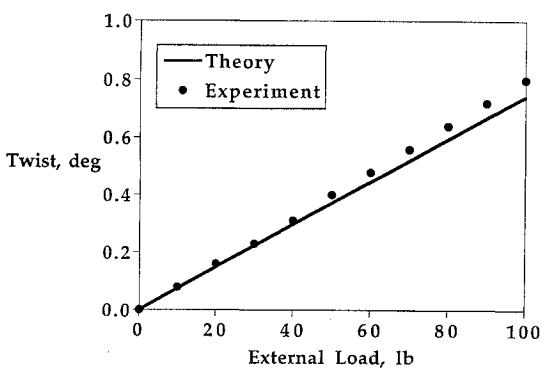

Fig. 13 Tip twist of $[20/-70]_s$ Kevlar-epoxy tube (l = 34.375 in., D = 1.57 in.) at different loads.

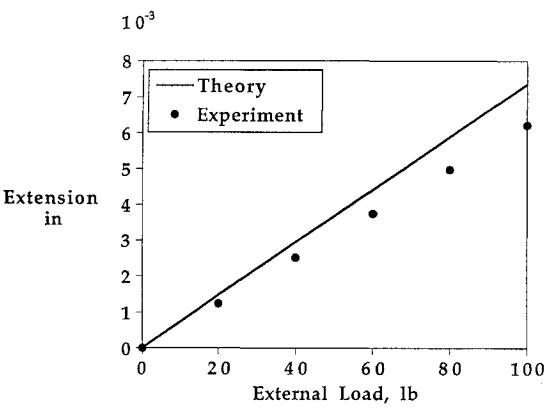

Fig. 14 Extension of $[20/-70]_s$ Kevlar-epoxy tube (l = 34.375 in., D = 1.57 in.) at different loads.

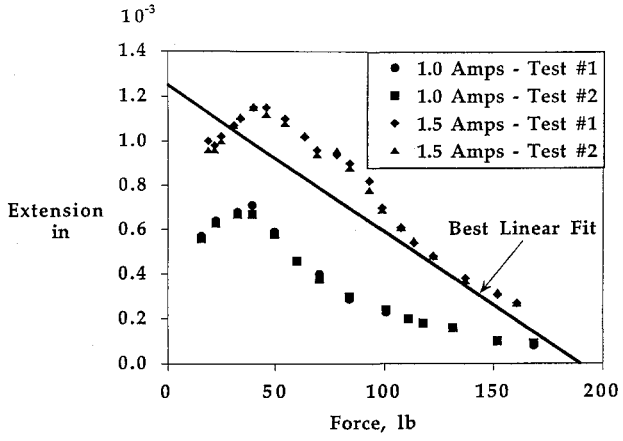

Fig. 15 Experimentally determined force-displacement curve of magnetostrictive actuator.

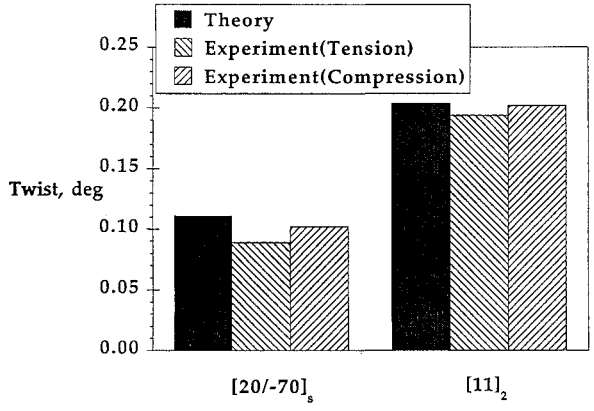

Fig. 16 Tip twist of $[20/-70]_s$ and $[11]_2$ Kevlar-epoxy tube with actuator (l = 34.375 in., D = 1.57 in.).

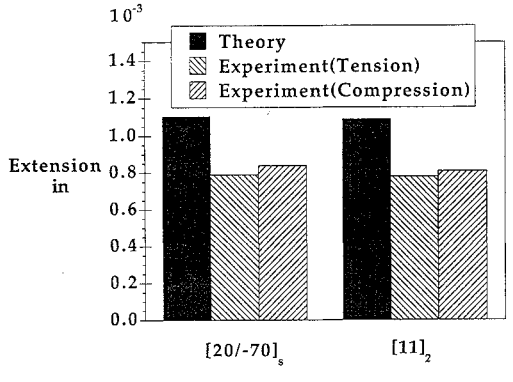

Fig. 17 Axial displacement of $[20/-70]_s$ and $[11]_2$ Kevlar-epoxy tube with actuator (l = 34.375 in., D = 1.57 in.).

experiment and prediction is within 5%. The axial force corresponding to 0.2 deg of twist is about 16 lb.

Figure 17 shows the comparison of predicted and experimental values of axial extension for the Kevlar-epoxy tube with actuator. The $[20/-70]_s$ Kevlar-epoxy tube system undergoes extensions of 0.79 mils and −0.84 mils in tension and compression, respectively. Both values are about 70% of the theoretical prediction of 1.11 mils. For the $[11]_2$ tube/actuator system, the measured displacement of the tube is 0.78 mils in tension and −0.81 mils in compression. Both values are again approximately 70% of the predicted value.

Alternate Actuator Concepts

The analysis carried out in this study is not limited to the use of magnetostrictive actuators in the actuator/tube system. This investigation shows that twist, force, and axial extension predictions for any

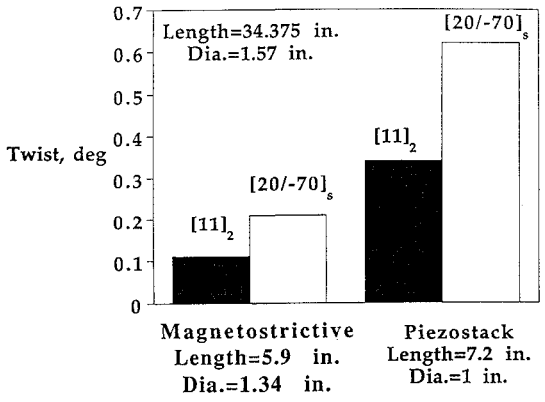

Fig. 18 Tip twist of Kevlar-epoxy composite tubes activated by magnetostrictive or piezostack actuator.

tube/actuator assembly can be made as long as the block force and free displacement of the actuator are known and the displacement compatibility is satisfied (i.e., the actuator is mechanically linked to the tube in such a way that the actuator stroke will equal the tube axial displacement). Based on the characteristics supplied by the manufacturer, both electrostrictive and piezoelectric stack actuators were considered as viable alternatives to the magnetostrictive actuator used in this study. It is to be noted here that the study using alternative actuators is confined to predictions only, as these actuators are not available in the dimensions suitable for present tubes.

Composite Tubes with Piezoelectric Stack Actuators

These actuators consist of thin piezoelectric sheets bonded together by a thin conducting epoxy. Voltage is applied by means of electrodes attached to the ends of the stack, causing the individual piezoelectric layers to expand across the thickness, thereby resulting in the elongation of the entire stack. These actuators also utilize a prestressing device in order to generate bidirectional motion. Compression can also be attained using a negative voltage; however, the stack is brittle in compression and may crack. The actuator selected for the numerical experiment has a block force of 787 lb and a free displacement of 3.54 mils at 1000 V. In a thermally stable $[20/-70]_s$ Kevlar-epoxy tube (length and diameter of 34.375 and 1.57 in., respectively), a tip twist of 0.34 deg and an axial force of 45 lb due to this actuator are predicted, whereas for the $[11]_2$ Kevlar-epoxy tube system (same tube dimensions as above), replacing the magnetostrictive actuator with the above piezoelectric stack actuator results in a predicted twist of 0.62 deg and a corresponding force of 51.4 lb, both about 3 times the values corresponding to magnetostrictive actuator. Figure 18 shows these results in a graphical form.

Composite Tubes with Electrostrictive Actuators

The operation of electrostrictive actuators is very similar to magnetostrictive actuators. The electrostrictive material will strain when an electric field is applied, as opposed to the magnetostrictive terfenol-D, which strains under a magnetic field. The electrostrictive actuators also use biasing in order to generate bidirectional motion. One actuator used in the present numerical study is 0.236 in. in diameter and 0.787 in. in length and has a block force of 450 lb and a free displacement of 0.75 mils. This actuator coupled with a $[11]_2$ Kevlar-epoxy tube of 10 in. length and 0.25 in. diam would generate a twist of 0.8 deg and axial force of 6.7 lb. Comparison of twist induced by electrostrictive, piezostack, and magnetostrictive actuators on the above-mentioned Kevlar-epoxy tube reveals the superiority of electrostrictive and piezostack actuators to the magnetostrictive actuator. The performances of electrostrictive and piezostack, however, are comparable to each other. Figure 19 shows these results in graphical form. Note that the performance of electrostrictive actuators degrades with the temperature, and hence this actuator is not suited for high-temperature applications.

Various configurations of Kevlar-epoxy composite tubes with different actuators for both maximum twist and axial force were

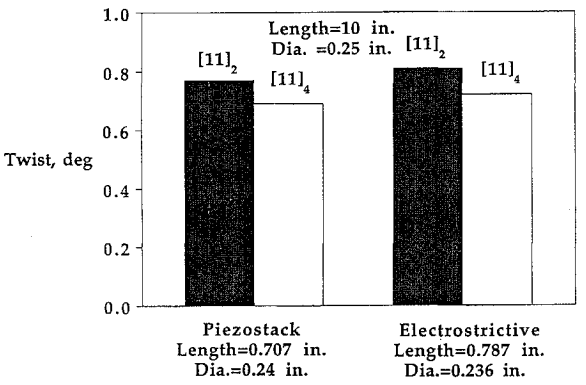

Fig. 19 Tip twist of Kevlar-epoxy tubes activated by piezoelectric stack or electrostrictive actuator.

examined. A 20-in.-long, 1.57-in.-diam $[11]_4$ Kevlar-epoxy tube with a magnetostrictive actuator resulted in induced twist of approximately 0.17 deg and axial force of 48 lb. Whereas the same tube with a suitable piezoelectric stack actuator would result in a predicted twist of 0.52 deg and an axial force of 154 lb.

For a full-scale flap application, the length of the system can be as large as 200 in., the axial force in the system must be high enough to counteract aerodynamic loads, and the flap deflection should be of the order of ± 8 deg in order to effectively reduce vibration. Based on the above tube/magnetostrictive actuator system design, ten $[11]_4$ Kevlar-epoxy tube/actuator systems of 20 in. length in series would generate approximately ± 1.7 deg of flap deflection and 48 lb of axial loading, as opposed to ± 5.2 deg of flap deflection and 154 lb of axial loading using piezoelectric stack actuators in an identical series of composite tube assemblies. To enhance the induced twist further, the use of smaller diameter tubes with piezostack actuators was theoretically examined. It was found that Kevlar-epoxy tubes of 10 in. length, 0.25 in. diam, and 0.02 in. thickness will generate a twist of 0.8 deg. Twenty such tubes in series can in principle produce 16 deg twist. Future research will focus on developing a multiobjective function study to optimize the tube/actuator design (type of actuator as well as tube size and lay-up) based on full-scale deflections and aerodynamic forces.

Conclusions

A methodology to predict twist and axial force in an extension-torsion coupled composite tube due to a linear actuation (magnetostrictive, piezoelectric stack, and electrostrictive) is developed. The predictions are experimentally validated. Good correlation between theory and experiment for induced twist is achieved. However, the predicted axial displacements do not correlate well with the experimental data.

The performance of piezostack, electrostrictive, and magnetostrictive actuators for the present application was evaluated by comparing the induced-twist prediction in Kevlar-epoxy $[11]_4$ tubes of 10 in. length, 0.25 in. diam, and 0.04 in. thickness. The comparison revealed the superiority of piezostack actuators to induce twist in extension-torsion coupled composite tubes.

Acknowledgments

This work was supported by the Army Research Office under grant DAAL 03-92-G-0121 with Gary Anderson as technical monitor. The authors also thank Kwok Yu and Jon Velapoldi for their assistance in manufacturing and testing of composite tubes.

References

[1]Chopra, I., and McCloud III, J. C., "A Numerical Simulation Study of Open-Loop, Closed-Loop and Adaptive Multicycle Control Systems," *Journal of the American Helicopter Society*, Vol. 28, No. 1, 1983, pp. 311–325.

[2]Ham, N., Behal, B., and McKillip, R., Jr., "Helicopter Rotor Lag Damping Augmentation Through Individual Blade Control," *Vertica*, Vol. 7, No. 4, 1983, pp. 361–371.

[3]Straub, F. K., and Robinson, L. H., "Dynamics of a Rotor with Nonharmonic Control," *Proceedings of the Forty-Ninth Annual American Helicopter Society Forum* (St. Louis, MO), May 1993.

[4]Dawson, S., and Straub, F. K., "Design, Validation, and Test of a Model Rotor with Tip Mounted Active Flaps," *Proceedings of the Fiftieth Annual American Helicopter Society Forum*, Washington, DC, 1994, pp. 361–372.

[5]Straub, F. K., and Merkley, D. J., "Design of a Servo-Flap Rotor for Reduced Control Loads," *Proceedings of the Fiftieth Annual American Helicopter Society Forum*, Washington, DC, 1994, pp. 305–314.

[6]Chen, P. C., and Chopra, I., "A Feasibility Study to Build a Smart Rotor: Induced-Strain Actuation of Airfoil Twisting Using Piezoceramic Crystals," paper presented at the SPIE's North American Conference on Smart Structures and Materials, Albuquerque, NM, Feb. 1993, pp. 234–254.

[7]Chen, P. C., and Chopra, I., "Induced Strain Actuation of Composite Beams and Rotor Blades with Embedded Piezoceramic Elements," paper presented at the SPIE's North American Conference on Smart Structures and Materials, Orlando, FL, Feb. 1994, pp. 123–190.

[8]Samak, D. K., and Chopra, I., "A Feasibility Study to Build a Smart Rotor: Trailing Edge Flap Actuation," paper presented at the SPIE's North American Conference on Smart Structures and Materials, Albuquerque, NM, Feb. 1993, pp. 225–237.

[9]Walz, C., and Chopra, I., "Design and Testing of a Helicopter Rotor Model with Smart Trailing Edge Flaps," *Proceedings of the AIAA/ASME/ASCE/AHS/ASC 35th Structures, Structural Dynamics, and Materials Conference* (Hilton Head, SC), AIAA, Washington, DC, 1994, pp. 309–319 (AIAA Paper 94-1767).

[10]Fenn, R. C., Downer, J. R., Bushko, D. A., Gondhalekar, V., and Ham, N. D., "Terfenol-D Driven Flaps for Helicopter Vibration Reduction," paper presented at the SPIE's North American Conference on Smart Structures and Materials, Albuquerque, NM, Feb. 1993, pp. 407–418.

[11]Chandra, R., and Chopra, I., "Structural Behavior of Two-Cell Composite Rotor Blades with Elastic Couplings," *AIAA Journal*, Vol. 30, No. 12, 1992, pp. 2914–2921.

[12]Winckler, S. J., "Hygrothermally Curvature Stable Laminates with Tension-Torsion Coupling," *Journal of the American Helicopter Society*, Vol. 30, No. 3, 1985, pp. 56–58.

[13]Samak, D. K., and Chopra, I., "Design of High Force, High Displacement Actuators for Helicopter Rotors," paper presented at the SPIE's North American Conference on Smart Structures and Materials, Orlando, FL, Feb. 1994, pp. 86–98.